Comparative Medicine
Copyright 2001
by the American Association for Laboratory Animal Science

Vol 51, No 6
December 2001
504-512

Evaluation of the Rat Stifle Joint After Transection of the Cranial Cruciate Ligament and Partial Medial Meniscectomy

Siyami Karahan, DVM,[1*] Steven Alan Kincaid, DVM, PhD,[1] John Robert Kammermann,[1] and James Carroll Wright, DVM, PhD[2]

Osteoarthritis (OA) was induced in the rat stifle joint by partial medial meniscectomy (PMM) and transection of the cranial cruciate ligament (CCL). At 10 weeks after destabilization, joint morphologic and pathologic changes were observed, scored, and compared. The intact rat stifle joint was observed in a mid-saggital plane. Articular cartilage of the distal portion of the femur and proximal portion of the tibia had thicker and thinner sites, and the thicker sites were located caudally on the distal portion of the femur and centrally on the proximal portion of the tibia. The two separate triangular portions of the medial meniscus observed in the mid-saggital plane contained a center of ossification in the cranial portion and fibrocartilage in the caudal portion. The synovium was one to three cells thick, and contained rare inflammatory cells. Although lesions were more severe in stifles after PMM, both treatments produced OA lesions that closely simulated OA lesions of other species. Lesions consistent with idiopathic OA included chondrocytic clones with increased metachromasia around them, chondrocytic death, loss of metachromasia, fibrillation, fissuring, erosion of articular cartilage, osteophyte formation, and variable synovial inflammation. The results indicate that PMM and CCL transection in the rat are useful in vivo models for study of the etiopathogenesis of OA and therapeutic efficacy of anti-arthritic drugs and treatment concepts.

In vivo animal models play integral roles in unraveling the complex interactions of biochemical, physiologic, and mechanical factors in the etiopathogenesis and therapy of osteoarthritis (OA) (1). Numerous models that are used to study OA are unified by their failure to mimic all aspects of human OA (2). Reviewers of OA models have characterized and classified various models, emphasizing their advantages and disadvantages (3, 4). Although canine models are most desirable, small laboratory animals such as the rat have some advantages over other experimental animals due in part to their low cost, ease of handling, and resistance to postsurgical infections (2, 5, 6). Also, many research diagnostic and analytical procedures, including antibodies, have been developed specifically for use in small rodents. The stifle joint of the rat may be particularly advantageous since it is sufficiently large to permit intra-articular injection, in vivo imaging, and gross necropsy evaluation (7, 8).

Transection of the cranial cruciate ligament (CCL) and meniscectomy were developed as early joint instability models to induce OA lesions (2, 9-12). Although CCL transection is the most common model of OA, partial resection of the medial meniscus mimics articular lesions observed after naturally acquired meniscal damage and OA (1, 13). Lesions induced by transection of the rat CCL included surface disruptions that extended deep into the articular cartilage, loss of complex sugars (proteoglycans), and chondrocyte death with clone formations (5). Osteophytes did not form during the short duration (four weeks) of this study; however, osteophyte formation was reported in a separate study (14). In other species, lesions induced by partial or complete meniscectomy were similar to those resulting from CCL transection, although the location of lesions was variable (9). However, reports regarding the effect of partial meniscectomy (PMM) in the rat were not found in published literature.

The histologic description of articular cartilage of the normal rat is limited and incomplete (5, 15-18). Comprehensive knowledge of the rat stifle joint is a prerequisite for interpretation of pathologic lesions that develop after destabilization of the joint. The study reported here was conducted to: describe the normal histologic structure and histochemical nature of articular cartilage of the rat stifle joint, compare lesions of OA that develop after transection of the CCL with those resulting from PMM of the medial meniscus of the rat, and determine whether OA lesions change following a long period after joint destabilization of the rat stifle joint.

Materials and Methods

The study was conducted under a protocol approved by the Auburn University Institutional Animal Care and Use Committee. Twenty-four adult male Wistar rats (*Rattus norvegicus*), weighing 375 to 400 g, between the ages of 120 and 140 days, were purchased by the Department of Laboratory Animal Health, College of Veterinary Medicine, from a USDA-licensed vendor (Harlan, Indianapolis, Ind.). On receipt, the rats were given a physical examination and were housed individually in standard shoe box-type cages (48 cm long, 25 cm wide, 20 cm deep, and 920 cm^2 in floor area). A commercially formulated diet (5P00 Prolab RMH 3000, PMI International, Inc., P.O. Box 19798, Brentwood, Mo.) and water were provided ad libitum. Husbandry and treatment of the rats were in accordance with the standard operating procedures of the Department of Laboratory Animal Health, College of Veterinary Medicine, Auburn University, and *The Guide for the Use and Care of Laboratory Ani-*

Received: 7/18/01. Revision requested: 8/28/01. Accepted: 9/19/01.
[1]Departments of Anatomy, Physiology, and Pharmacology and [2]Pathobiology, 109 Greene Hall, College of Veterinary Medicine, Auburn University, Alabama, 36849.
[*]Corresponding author.

mals. After allowing two weeks for the rats to adapt to the housing environment, they were assigned randomly to one of three groups of seven rats each: group 1, untreated controls; group 2, treatment by PMM; and group 3, treatment by CCL transection.

On day 0, PMM and transection of the CCL of the left stifle joint of rats in groups 2 and 3, respectively, were performed. Anesthesia for each rat was initiated with halothane (Fort Dodge Animal Health, Fort Dodge, Iowa) and was maintained by intra-peritoneally injected sodium pentobarbital (50 mg/kg of body weight; The Butler Company, Columbus, Ohio). Transection of the CCL was accomplished, using the aseptic procedure described by Williams and co-workers (5).

The same surgical approach was used to expose of the medial meniscus of rats in group 2. The medial meniscus was gently retracted, and the cranial third was carefully excised by use of a Dumont hard carbon steel cutter (Fine Science Tools Inc, Foster City, Calif.) to ensure that the articular surface of the femur and tibia were not damaged. The joint capsule was closed, using 5-0 Dexon absorbable sutures. After opposing the musculature, the skin was sutured, using a simple interrupted pattern.

Rats of all groups were euthanatized by administration of a concentrated sodium pentobarbital euthanasia solution (^{6}Socum B-6 Gr, The Butler Company, Columbus, Ohio) on day 84. Each stifle joint was excised in toto by transection at the midshaft of the femur and the tibia. The excised joint was immediately placed in buffered 10% formalin. After decalcification, specimens were processed in paraffin and embedded. The embedded samples were serially sectioned on a rotary microtome at a thickness of 5 μm. Every ninth and tenth slide was stained with hematoxylin & eosin and toluidine blue, respectively, and blindly evaluated by use of light microscopy. Microscopic analysis of the stifle joint was conducted, using a mid-sagittal section of the medial condyle of the distal portion of the femur and corresponding to the medial condyle of the proximal portion of the tibia.

The location of analysis was standardized by observing the triangular shape of the cranial and caudal portions of the medial meniscus in serial sections just prior to the presence of articular cartilage of the patellar groove. Articular cartilage of the distal portion of the femur and proximal portion of the tibia was divided into five regions for analysis (Fig. 1). Region 1 was located at the cranial margin, region 2 was in contact with the cranial portion of the medial meniscus, region 3 was in the central area of the joint, region 4 was contact surface with the caudal portion of the medial meniscus, and region 5 was located at the caudal margin.

Statistical analysis. In addition to describing histomorphologic and histopathologic changes, lesions were numerically scored (Table 1). The total articular cartilage score and osteophyte formation were analyzed by use of analysis of variance (ANOVA) for ranked data and the least significant difference (LSD) for multiple comparisons. Synovitis was analyzed, using the general linear model (GLM) for ranked data and Scheffé's test for multiple comparisons. For the multiple comparison tests, $P \leq 0.05$ was considered significant. Multiplication of the tidemark was analyzed, using a categorical model and multiple contrast to compare regions. All data analysis was conducted, using statistical analysis system (SAS) software (release version 6.12, SAS Institute, Inc., Cary, N.C.).

Results

Postsurgical recovery of all rats was unremarkable.

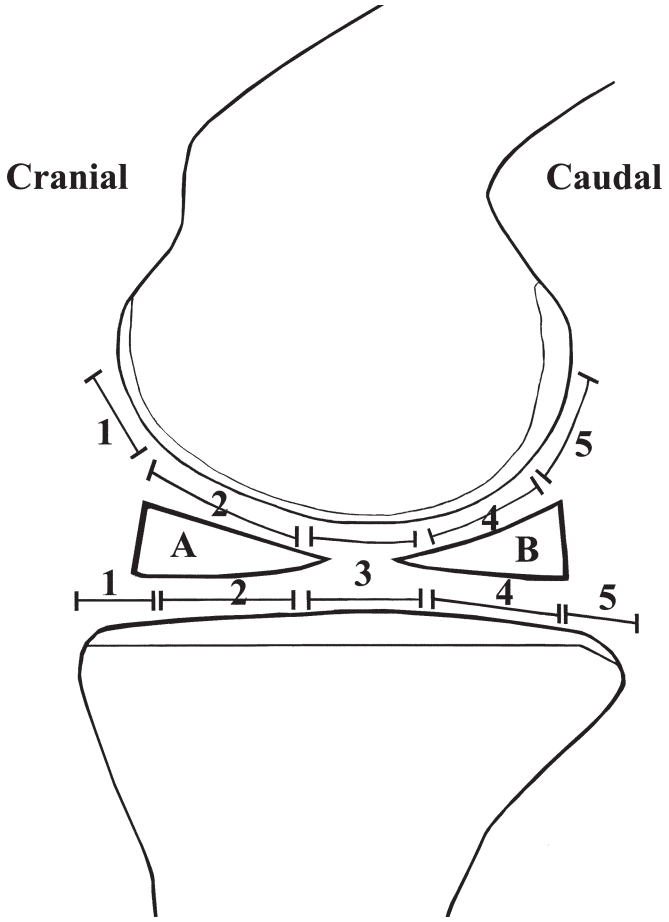

Figure 1. Anatomic location for analysis of the rat stifle joint in sagittal sections was standardized by observing the triangular shape of the cranial (A) and caudal (B) portions of the medial meniscus. Articular cartilage of the distal portion of the femur and proximal portion of the tibia was divided into five regions. Region 1 was located at the cranial margin, region 2 was in contact with the cranial portion of the medial meniscus, region 3 was in the central area of the joint, region 4 was contact surface with the caudal portion of the medial meniscus, and region 5 was located at the caudal margin.

Group 1 (control). Non-calcified and calcified portions of articular cartilage of the distal portion of the femur and proximal portion of the tibia were separated by a basophilic tidemark (Fig. 2A). Thickness of non-calcified and calcified cartilages on the distal femoral condyle were similar or the calcified cartilage was slightly thicker (Fig. 2A and 2C). However, in regions 4 and 5, the non-calcified cartilage was thicker than the calcified cartilage (Fig. 2A). Non-calcified articular cartilage was thicker on the proximal portion of the tibia, except near joint margins where it approximated the thickness of calcified cartilage (Fig. 2A and 2D). Thickness of non-calcified tibial cartilage was greatest in region 3 (Fig. 2A).

The non-calcified articular cartilage was morphologically divisible into a superficial tangential layer, an intermediate layer, and a deep layer. The surface of articular cartilage of the distal portion of the femur and proximal portion of the tibia had a thin line of eosinophilia that rarely was penetrated by superficial fibrillations. The gray to lightly eosinophilic interterritorial matrix of the superficial and intermediate layers was more eosin-

Table 1. Scoring scale for lesions of the rat stifle

Articular cartilage (0-20)
Structure 0 = Normal 1 = Slight surface erosion or flaking of superficial zone 2 = Erosion no deeper than superficial zone 3 = Erosion into middle zone with or without fissuring 4 = Erosion into deep zone with or without fissuring 5 = Erosion into calcified zone 6 = Erosion into the subchondral bone (eburnation) 7 = Fibrous tissue on eburnated areas
Tidemark 0 = Normal 1 = Touched by blood vessels 2 = Crossed by blood vessels
Doubling of tidemark 0 = Normal (a basophilic line) 1 = Doubled
Metachromatic staining 0 = Normal 1 = Increased in all layers of articular cartilage 2 = Significantly decreased or no deeper than superficial zone 3 = Significantly decreased or absent, no deeper than middle zone 4 = Significantly decreased or absent no deeper than tidemark 5 = No staining at all
Chondrocyte morphology 0 = Normal 1 = Enlarged cells close to the surface of articular cartilage 2 = Hypercellular with or without small clones 3 = Noticeable hypocellularity with or without clones 4 = Significant hypocellularity with or without clones 5 = Severe hypocellularity
Osteophyte formation (0–2) 0 = None 1 = Extensive mix tissue formation and remodeling at joint margin 2 = Osteophyte
Synovitis (0–4) 0 = Norma1 (1- to 3-cell-thick synovium and few mononuclear cells in subintima) 1 = Slight increase in number of synoviocytes and mononuclear cells 2 = Mononuclear cell infiltration and hyperemic blood vessels 3 = Hyperplastic synovium 4 = Extensive hyperplasia with pannus formation

ophilic, with greater spacing between chondrocytes in the deep layer. This morphology was more conspicuous in the proximal portion of the tibia (Fig. 2D). Territorial matrices were darker in the intermediate and deep layers (Fig. 2D). Blood vessels were not penetrating the tidemark of either the distal portion of the femur or proximal portion of the tibia. Although multiple tidemarks were present in articular cartilage of both joint surfaces (Fig. 2C), they were significantly ($P = 0.0001$) less frequent in region 3 of the proximal portion of the tibia and regions 4 and 5 of the distal portion of the femur (Fig. 2D).

Superficial chondrocytes in the articular cartilage usually were lenticular in shape, except in region 3 where they were oval. This was more pronounced in the proximal portion of the tibia (Fig. 2D). The remainder of the non-calcified cartilage contained round chondrocytes that were organized into columns adjacent to the tidemark (Fig. 2D). Columnization in the distal portion of the femur was less conspicuous than that in the proximal portion of the tibia (Fig. 2C), except in thick articular cartilage of the condyle. In the proximal portion of the tibia, round chondrocytes in the intermediate layer and adjacent portions of the superficial layer were larger than those in the rest of the non-calcified articular cartilage and those of the femur (Fig. 2D). In addition, femoral chondrocytes had little variability in size (Fig. 2C). Regardless of the location, the largest chondrocytes were localized in the layers of calcified cartilage near the subchondral bone (Fig. 2C and 2D). Chondrocytic clones were rarely observed in the intermediate layer of either the femur or tibia.

Metachromatic staining was uniform throughout the articular cartilage of the distal portion of the femur and proximal portion of the tibia (Fig. 2B). However, loss of metachromasia was evident in the superficial tangential layer of the proximal portion of the tibia. Metachromasia, especially in the territorial matrices, was more intense in the deep layer, although it also increased in region 3 of the distal portion of the femur and proximal portion of the tibia.

The cranial and caudal portions of the medial meniscus had a triangular shape (Fig. 2A and 2B). Although a focus of ossification surrounded by large chondrocytes was present in the cranial portion, the caudal portion only contained fibrocartilage (Fig. 2A and 2B). The intima of the synovial membrane was one to three cells thick and was supported by a subintima that contained a few inflammatory cells.

Group 2 (PMM, left stifle). A small piece of the cranial portion of the medial meniscus was observed, and the excised portion was replaced partially by fibrous connective tissue. Fibrillations accompanied by a few tears were observed in the caudal portion.

Lesions were significant ($P \leq 0.05$) in the distal portion of the femur, compared with those in controls, and they were significantly ($P \leq 0.05$) more severe in regions 1-3 (Fig. 3A; Table 2). A layer of fibrocartilage covered articular cartilage of region 1 and adjacent portions of region 2 (Fig. 3A), and frequently contained chondrocytic clones. Loose connective tissue often rich in cells and capillaries was located just beneath the fibrocartilage and in several regions of the subchondral bone (Fig. 3A). Although the laminar architecture of articular cartilage was discernable, chondrocytes and matrical metachromasia were absent in regions 1, 2, and 3 of the medial femoral condyle (Fig. 3A and 4A). Fibrillation and fissuring of articular cartilage in region 2 progressed to erosion of non-calcified cartilage in region 3. Matrical eosinophilia, which corresponded to loss of metachromasia, and hypocellularity also were apparent in region 4 (Fig. 3A and 4A). Articular cartilage of region 5 was hypercellular, but chondrocytes were randomly arranged rather than aligned in columns as observed in control tissue. Large and small chondrocytic clones with increased territorial basophilia were observed. The absence of metachromasia in regions 1-3 was replaced by a gradual increase in staining intensity in region 4 until it was greatest around clones in region 5 (Fig. 4A). Blood vessels penetrated articular cartilage in regions 1 and 2 and the adjacent portion of region 3. Multiple tidemarks were frequent in all regions including 4 and 5, with no significant ($P > 0.05$) difference among any regions. Chondrophytes were observed at the margin of region 5 in the articular cartilage-synovial membrane junction. (Fig. 3F).

Lesions of the articular cartilage of the proximal portion of the tibia were significant ($P \leq 0.05$), compared with those of groups 1 and 3 and were more severe than those of the distal portion of the femur (Fig. 3A). A pannus-like fibrous membrane was attached to the articular surface in region 1 (Fig. 3C). Complete erosion of articular cartilage to subchondral bone was evident in region 3 (Fig. 3A). Gradual loss of metachromasia in the joint surface extended from joint margins to region 3. Concomitant fibrillation of the articular surface changed to fissuring with hypocellularity (Fig. 3A and 4B). Articular cartilage caudal to region 3 had a gradual increase in metachromasia and chon-

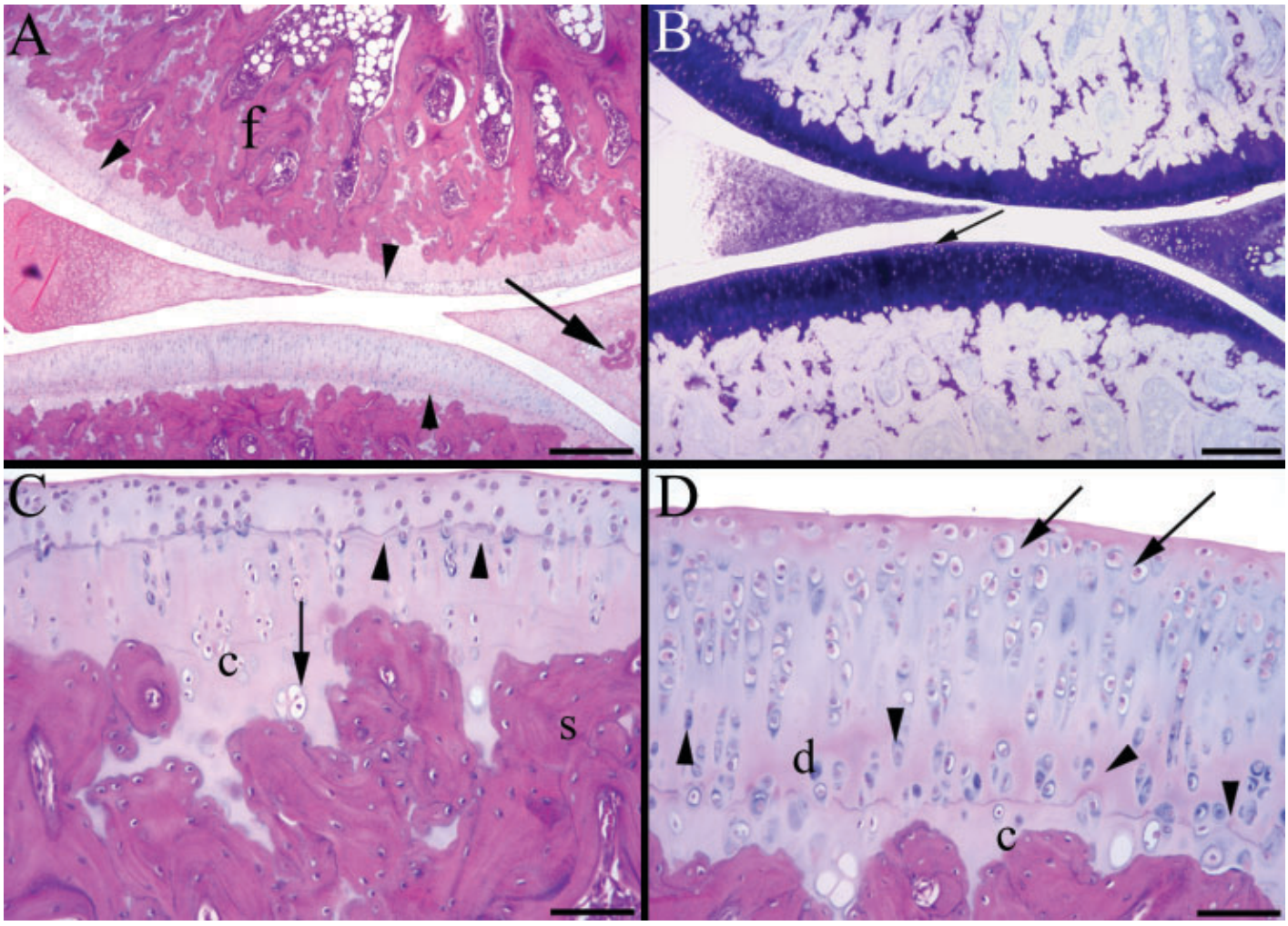

Figure 2. Photomicrographs illustrating the normal microscopic features of sections of articular cartilage of the distal portion of the femur and proximal portion of the tibia of the adult rat. (A) Articular cartilage of the distal portion of the femur (f) and proximal portion of the tibia (t) is separated into non-calcified and calcified portions by a basophilic tidemark (arrowheads). On the femur, thickness of non-calcified and calcified cartilages was similar or the calcified cartilage was slightly thicker. However, in regions 4 and 5 the non-calcified cartilage is thicker than the calcified cartilage. On the tibia, non-calcified articular cartilage is thicker except near joint margins where it approximated the thickness of calcified cartilage. The cranial and caudal portions of the medial meniscus were triangular in shape. A center of ossification (arrow) surrounded by large chondrocytes is present in the cranial portion, and the caudal portion is composed of fibrocartilage. (B) Metachromatic staining of articular cartilage of the distal portion of the femur and proximal portion of the tibia is uniform; however, there is slight loss of metachromasia at the surface of the tibia (arrow). (C) The lenticular chondrocytes at the surface of the distal portion of the femur become round and randomly distributed in rest of the non-calcified cartilage. The most hypertrophic chondrocytes (arrow) are located in the calcified cartilage (c), near the subchondral bone(s). Multiple tidemarks (arrow heads) can be observed in this photomicrograph taken from region 3. (D) Chondrocytes are oval at the surface of the proximal portion of the tibia in region 3 and organized into columns in rest of the non-calcified cartilage. Except for the most hypertrophic chondrocytes of the calcified cartilage (c), the largest chondrocytes (arrows) are located in the upper part of the middle layer of the non-calcified cartilage. A dark basophilic territorial matrix (arrowheads) surrounds the chondrocytes of the deep and the middle layers. H&E (A, C, and D) and toluidine blue (B) stains; bar = 400 μm in A and B and 100 μm in C and D.

drocytic clone formation (Fig. 4B and 4D). Vascular invasion through the tidemark was prominent in regions 1 and 3 (Fig. 4C). Multiple tidemarks were common in every regions except region 3, where complete erosion was observed. Osteophyte numbers were significant ($P \leq 0.05$), compared with those of controls, and they were more frequent at the caudal margin.

Mononuclear inflammatory cells and congested blood vessels represented an inflammatory response in the synovium that was significant ($P \leq 0.05$), compared with that of groups 1 and 3 (Table 4). The inflammatory response was significantly ($P \leq 0.05$) higher in the cranial part of the synovium where synovial hyperplasia with increased synovial villi and folds, as well as pannus formation, was observed (Fig. 3C).

Group 3 (CCL, left stifle). Lesions of the distal portion of the femur resulting from transection of the CCL also were significant ($P \leq 0.05$), compared with those of controls, were similar to those described for group 2, and were concentrated in articular cartilage of regions 1, 2, and 3 (Fig. 3B; Table 2). However, lesions did not extend as far into large areas of region 4 as they did in group 2. Articular cartilage in regions 4 and 5 was thick with clones and extensive metachromasia; however, fibrillations, pitting, and small fissures at the surface also were observed (Fig. 3B). Deep fissures

with adjacent clones were rarely observed in the region 4 (Fig. 3B and 4C). Blood vessels penetrated the tidemark in regions 1 and 2. However, multiple tidemarks were significantly ($P = 0.02$) less frequent in regions 1 and 2 where blood vessel invasion and cartilage damage occurred. Osteophyte formation at the cranial margin of the articular surface was significantly ($P \leq 0.05$) higher than that in groups 1 and 2 (Fig. 3E).

In the proximal portion of the tibia, lesions of the articular cartilage were significantly ($P \leq 0.05$) more severe than those of controls, but were significantly ($P \leq 0.05$) less severe than those of group 2 (Fig 3B). Osteophyte formation at the cranial joint margin was significant ($P \leq 0.05$), compared with that of controls; however, it was not significant ($P > 0.05$), compared with that of group 2 (Fig 3D). Vascular invasion through the tidemark into articular cartilage was frequently observed at the cranial joint margin (Fig 3D). The articular surface was fibrillated, with decreased metachromasia. Multiple tidemarks were present throughout the cartilage; however, they were significantly ($P = 0.0001$) less frequent in regions 2 and 3.

The medial meniscus had surface fibrillations with a few tears that were more prominent in the cranial portion (Fig. 3B). Inflammation in the synovial membrane was significant ($P \leq 0.05$), compared with that of controls and was less significant ($P \leq 0.05$), compared with that of group 2; its severity was greater in the cranial region (Fig. 3D, Table 4).

Discussion

In general, the morphology and chemical composition of normal articular cartilage is similar among animal species (19). However, differences exist within a species or an individual joint (15). Such differences are exemplified by the thickness of articular cartilage, which has a direct relationship to body weight (16). Thus, articular cartilage of the rat is thin, compared with that of larger species, but it has more cells per unit volume due to an inverse relationship between the thickness of articular cartilage and the number of resident chondrocytes (16). Also, the non-calcified articular cartilage of the rat had regional variations in thickness on the distal portion of the femur and proximal portion of the tibia. Articular cartilage located on the caudal distal portion of the femur and central portion of the tibia was thick. Conversely, calcified cartilage in these regions was thin. As reported by Thaxter and co-workers (20), regions of thick non-calcified articular cartilage on the proximal portion of the tibia and distal portion of the femur opposed each other when the rat stifle was in a naturally flexed position. A tidemark was observed between the non-calcified and calcified portion of articular cartilage of the distal portion of the femur and proximal portion of the tibia, as described in larger species (15).

As observed in humans and domestic animals, articular cartilage of the rat was divisible into four layers: superficial tangential layer, intermediate layer, deep layer, and calcified cartilage (5). Chondrocytes of the superficial layer are ellipsoidal in humans and lenticular or flat in laboratory animals, such as the rabbit, but they are round and large near the tidemark (15). Gyarmati and co-workers. (18) reported that chondrocytes in articular cartilage of the proximal portion of the tibia of old rats were hypertrophic in the intermediate layer, and their size was uniform throughout the cartilage. In the study reported here, chondrocytes were large in the intermediate layer and adjacent portion of the superficial layer as described by Gyarmati and co-workers. (18). However, chondrocytes in the deep layer were small, which resulted in more interterritorial matrix between chondrocytes of the deep layer. In this study, metachromatic staining of glycosaminoglycans was most abundant in the matrix of the intermediate layer and the territorial matrices of the deep layers, which reflects greater metabolic and synthetic activity of chondrocytes in these regions, compared with those of the remainder of the cartilage (21).

The rat meniscus is composed of hyaline cartilage and fibrocartilage, and is ossified in old animals (17, 22). Kiss and Földes (17) reported that hyaline cartilage was located in the medial meniscus and fibrocartilage was located in the lateral meniscus of the rat stifle. In this study, hyaline cartilage and fibrocartilage were located in the cranial and caudal portions of the medial meniscus, respectively. The difference between the observations in this study and those of Kiss and Földes (17) probably resulted from differences in specimen orientation. In our study, the intact rat stifle was serially sectioned in approximately a mid-sagittal plane of the medial femoral condyle. Consequently, only the cranial and caudal portions of the medial meniscus were visible. In the Kiss and Földes study (17), the entire rat stifle was "halved in a mid sagittal plane" and was prepared for histologic sections. This orientation would not allow observation of medial and lateral menisci within the same plane of section. Thus, cranial and caudal portions of either the medial or lateral meniscus were observed.

Osteoarthritis is not simply a "wear-tear disease" of articular cartilage, but is a dynamic series of complex events leading to the breakdown of the joint (23-25). Therefore, an experimental model for study of OA should simulate more aspects of the disease than simply destruction of articular cartilage (13). In this study, rat stifles treated by CCL transection or PMM developed degeneration of articular cartilage similar to that found in naturally acquired OA as well as lesions in the other joint tissues. Lesions included fibrillation and fissuring of the articular surface, loss of metachromasia, clones with increased metachromasia, chondrocytic death, joint remodeling with marginal osteophytes, joint capsule thickening, and synovial membrane inflammation. Although OA lesions were consistent within each model and were typical of OA lesions in other species, they differed in severity and anatomic location. Destabilization of the stifle by PMM resulted in more severe lesions than did CCL transection. Also, inflammation of the synovial membrane was greater in rats treated by PMM and was most pronounced in the cranial region of the joint. Although osteophytes were observed at the cranial joint margins of stifles with PMM, chondrophyte and osteophyte numbers were more significant at the caudal joint margin of the proximal portion of the tibia and distal portion of the femur, compared with those associated with the stifles that were treated by CCL transection. However, osteophyte numbers at the cranial joint margin of the distal portion of the femur and proximal portion of the tibia were greater in the stifles that were treated by CCL transection.

The etiopathogenesis of osteophytes has not been definitely clarified. In our study, chondrophytes at the caudal joint margin of the femoral condyle may have originated by hyperplasia of chondrocytes of the superficial layer (26). Vascular invasion of the chondrophytes suggested that they could progress to osteophytes, as reported in other species (9). As an alternative, Okazaki and co-workers (27) observed osteophyte formation from proliferation of

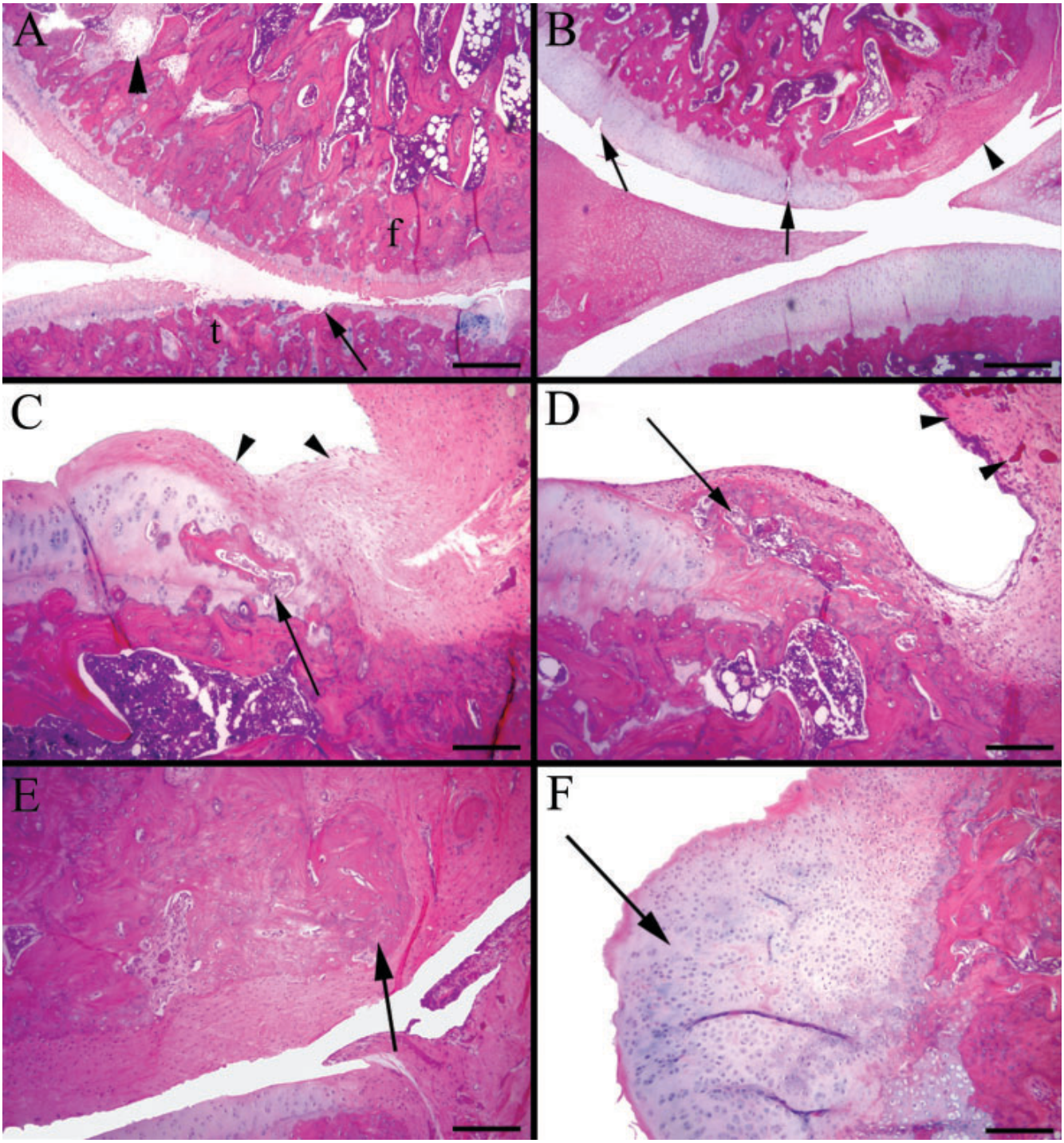

Figure 3. Photomicrographs of sections of the lesions resulting from partial medial meniscectomy (PMM) and transection of the cranial crucial ligament (CCL). (A) In PMM-treated stifles, severe lesions in regions 1, 2, and 3 of the distal portion of the femur (f) extended into region 4. Fibrillation and fissuring of articular cartilage in region 2 progressed to erosion of non-calcified cartilage in region 3. Region 4 is hypocellular, with loss of metachromasia. Loose connective tissue (arrowhead) was located in several regions of the subchondral bone. In the proximal portion of the tibia (t), lesions were more severe and concentrated in regions 2, 3, and 4. Complete erosion of articular cartilage to subchondral bone (arrow) was observed in region 3. (B) Lesions resulting from transection of the CCL were concentrated in articular cartilage of regions 1, 2, and 3 of the distal portion of the femur. Articular surface of regions 1 and 2 was occupied by a layer of fibrocartilage (arrowhead). Beneath the fibrocartilage, loose connective tissue rich in capillaries (white arrow) was often present. In regions 4 and 5, articular cartilage was thick with fibrillations, pitting, and fissures (arrows) at the surface. Lesions in the proximal portion of the tibia were considerably less severe. (C) Vascular invasion through the tidemark (arrow) is exemplified in this photomicrograph of regions 1 of the proximal tibia of the PMM-treated rat stifle. In PMM-treated stifles, synovial membrane at cranial joint margin was hyperplastic, with pannus formation (arrowheads). (D) Synovitis (arrowheads) with hyperemic blood vessels was also present in CCL-transected stifles, but it was not as severe as that of PMM-treated stifles. Osteophyte formation (arrow) at the cranial joint margin of the proximal portion of the tibia was associated with both treatments (E) A well developed osteophyte (arrow) from the cranial joint margin of the distal portion of the femur in stifles with transected CCL. (F) In PMM-treated stifles, chondrophytes (arrow) were observed at the caudal joint margin of the distal portion of the femur. H&E stain; bar = 400 μm in A and B, and 165 μm in C, D, E, and F.

Table 2. Comparison of articular cartilage scores among regions of the left joint within each group

	Group 1		Group 2		Group 3	
	D Femur	P Tibia	D Femur	P Tibia	D Femur	P Tibia
Region 1	1 (0, 2)	1^{b} (1, 3)	6^{a} (13, 18)	15^{a} (13, 18)	15^{a} (11, 16)	6 (2, 10)
Region 2	1 (0, 2)	1^{b} (0, 3)	13^{b} (7, 15)	11^{b} (7, 13)	11^{b} (9, 16)	5 (3, 8)
Region 3	2 (1, 2)	3^{a} (2, 5)	12^{b} (10, 15)	17^{a} (12, 18)	11^{b} (7, 16)	6 (5, 11)
Region 4	1 (1, 2)	3^{a} (1, 4)	11^{b} (9, 16)	11^{b} (8, 17)	7^{c} (2, 13)	5 (2, 12)
Region 5	1 (0, 3)	1^{b} (0, 3)	7^{c} (4, 8)	6^{c} (5, 7)	5^{c} (2, 7)	5 (2, 9)

Scores are expressed as median (minimal, maximal values). Medians with different superscripts are significantly different at $P \leq 0.05$ (analysis of variance [ANOVA] on ranked data with least significant difference [LSD] multiple comparisons).
D = distal portion; P = proximal portion.

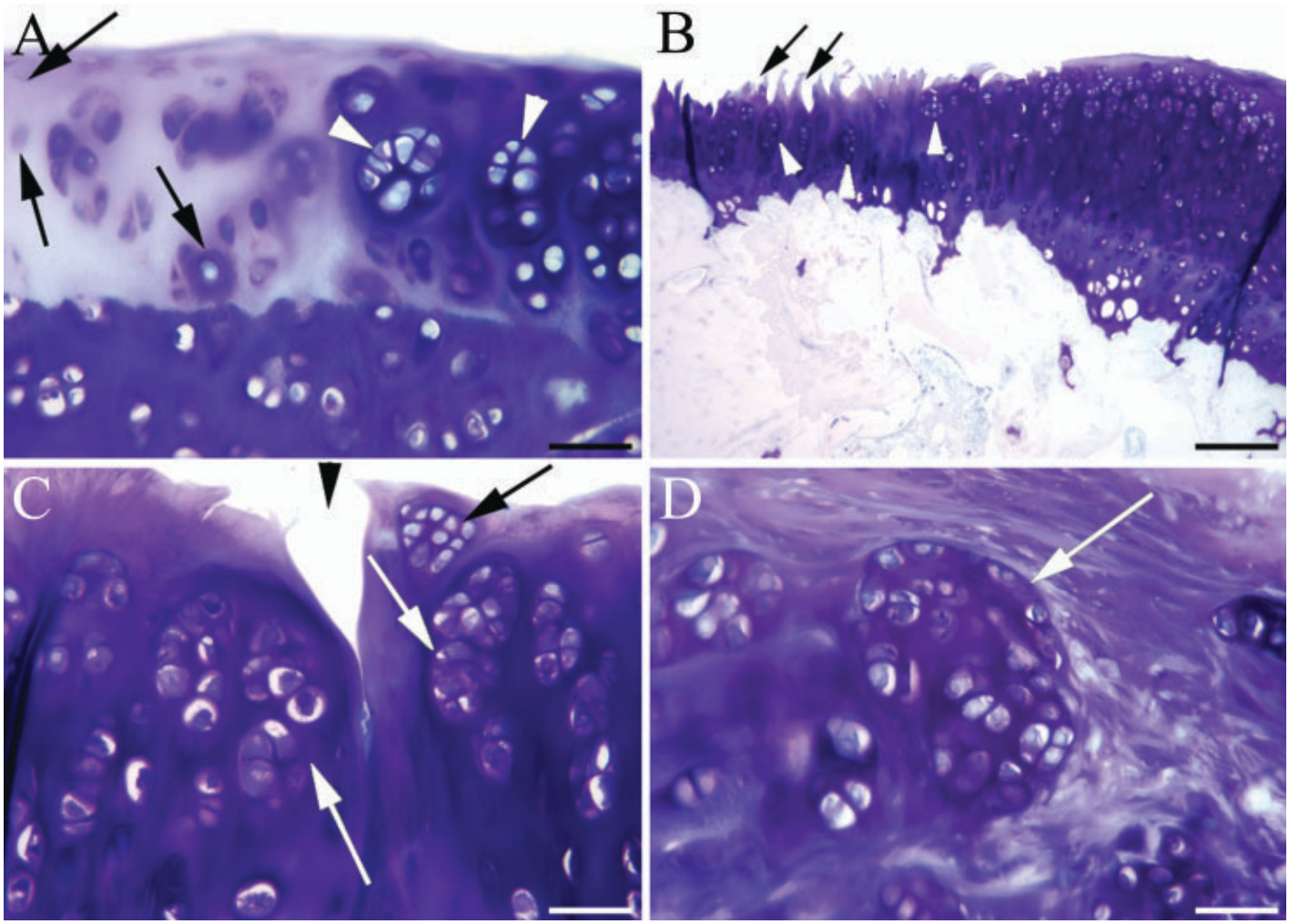

Figure 4. Photomicrographs of sections of the articular cartilage response illustrating metachromatic staining of the tissue. (A) Loss of metachromasia associated with chondrocytic death (arrows) was apparent in severe lesions. Metachromasia was great around chondrocytic clones (arrowheads) in cartilage adjacent to severely affected regions. This typical response is exemplified by this photomicrograph of region 4 of the distal portion of the femur treated by PMM. (B) In the proximal portion of the tibia treated by PMM, erosion of cartilage in region 3 was adjacent to fibrillation and fissuring (arrowheads) in region 4, which were usually contained clones (arrow) (C) Clones (arrows) were also associated with random deep fissures (arrowheads). (D) A giant clone (arrow) in region 4 of the proximal portion of the tibia treated by PMM exemplifies the chondrocytic effort to maintain matrix. Toluidine blue stain; bar = 40 μm in A, C, and D, and 165 μm in B.

synovial membrane and periarticular tissue followed by cartilage formation as a precursor to endochondral ossification. We also observed that a synovial membrane-like tissue covered osteophytes, especially at the cranial region of the femoral and tibial condyles. Vascular penetration from subchondral bone through the tidemark frequently was observed at sites where osteophytes developed, and in other regions where severe cartilage erosion was apparent. Regardless of their origin, formation of osteophytes is variable among joints and may be dependent on factors such as distribution of blood vessels in subchondral bone (11, 28).

Transection of the CCL in rats was studied by Williams and co-workers (5) for four weeks, with and without exercise. It induced surface disruptions that extended deep into articular cartilage in the exercised group, loss of resident complex sugars and chondrocytes, and formation of a few clones. However, osteophyte formation did not occur. In this study, degeneration of

Table 3. Comparison of total articular cartilage scores among groups

Group	Left femur	Left tibia	Left joint (overall)	Right femur	Right tibia
1	5[b] (4, 7)	9[c] (6, 13)	7[c] (4, 13)	8 (4, 10)	8[b] (7, 11)
2	58[a] (46, 67)	61[a] (48, 65)	59[a] (46, 67)	8 (7, 12)	13[a] (12, 16)
3	50[a] (39, 68)	27[b] (17, 41)	41[b] (17, 68)	7 (5, 8)	9[b] (5, 11)

Total scores of 5 regions are expressed as median (minimal, maximal values). Medians with different superscripts are significantly different at $P \leq 0.05$ (ANOVA on ranked data with LSD multiple comparisons).

articular cartilage was characterized by chondrocytic death, loss of metachromasia, and formation of large chondrocytic clones with increased territorial metachromasia at twelve weeks after CCL transection. Moreover, osteophytes formation occurred at the cranial joint margins.

Partial medial meniscectomy of the rabbit stifle joint resulted in lesions in articular cartilage of the femoral condyle as well as the tibial plateau (9). Osteophytes developed on the entire rim of the medial tibial plateau of the proximal portion of the tibia and on the medial femoral condyle. In this study, lesions in articular cartilage of the medial femoral condyle extended from the cranial to caudal regions of the articular surface and tibial lesions occupied a large area of the central region of the tibial plateau. Mid-sagittal histologic orientation used in this study allowed visualization of only the cranial and caudal margins of the articular surface. Thus, it was not possible to determine whether osteophytes formed along the medial surface of the tibial plateau. In the PMM rabbit model, inflammation of the synovium was mild or absent (9, 13). However, synovial membrane of the stifle of rats subjected to PMM had a prominent inflammatory response.

Iatrogenic models of OA commonly rely on the contralateral joint as a control (29, 30). The credibility of using such controls has been questioned on the basis of altered biomechanics between treated and untreated limbs (31). In the study reported here, the histologic morphology of right stifles of rats of groups 2 and 3 were similar to both stifles of the rats in group 1. However, minor histologic changes were apparent, compared with those of the right stifles of the control group (Table 3). In group-2 rats, articular cartilage of the proximal portion of the tibia had more hypertrophic cells and loss of metachromasia from the superficial layer of the region 3.

The pathogenesis of OA is biphasic, with compensatory and decompensatory components to the disease process (25). Lesions in both experimental groups of this study contained articular cartilage that manifested a panoramic view of the pathogenesis of OA. The morphology and histochemical nature of articular cartilage progressed from normal cartilage at the periphery of the joint surface through compensatory changes of thickening, clone formation and increased metachromasia, to the terminal events of decompensation in the area of the joint surface where chondrocytic death and matrix destruction predisposed development of an erosive OA lesion.

Duplication of the tidemark is observed in OA as well as normal articular cartilage (32). In this study, normal articular cartilage of the femoral condyle and tibial condyle had multiple tidemarks except in areas where non-calcified articular cartilage was thick. This probably represents a normal ongoing remodeling process in the rat stifle (32). The reliability of including duplication of the tidemark in scoring systems to diagnose OA is currently under discussion (33, 34). In this study, thick articular cartilage at the caudal region of the distomedial femoral condyle had multiple tidemark in rats of both treatment groups, which was not a feature of the control group. This was probably due to increased joint remodeling following the treatments. In all groups, delineation of multiple tidemarks of the articular cartilage covering the center of the proximal portion of the tibia was difficult due to the discrete calcified layer. Either multiplication of the tidemark never happened at this site, or if it did, it was replaced by subchondral bone during the ossification process.

Table 4. Comparison of synovitis in the left stifle joint among groups

Group	Cranial site	Caudal site	Overall
1	0[b] (0, 0)	0[c] (0, 1)	0[c] (0, 1)
2	4[a] (3, 4)	3[a] (2, 3)	3[a] (2, 4)
3	3[a] (3, 4)	2[b] (1, 3)	2[b] (1, 4)

Medians with different superscripts are significantly different at $P \leq 0.05$ (GLM on ranked data with Scheffé's test for multiple comparisons).

Articular cartilage has a limited capability of regeneration and repair (35, 36). Repair tissue can be observed on articular surfaces in later phases of degenerative joint diseases such as OA. This tissue may originate from synovium (37) or undifferentiated progenitor cells from the vasculatures in the subchondral bone (38). In this study, fibrocartilage was observed at the cranial margin of the femoral condyles of stifles of rats treated by PMM and CCL transection. A connective tissue rich in capillaries was located just beneath this fibrocartilage. The cranial end of this fibrocartilage also was associated with the synovium. We did not investigate the origin of this fibrocartilage; however, its presence may be a component of an early repair attempt to reestablish the integrity of the articular surface of the femoral condyle in conjunction with intrinsic regeneration suggested by increased metachromasia and clone formation.

In conclusion, destabilization of the rat stifle by PMM or CCL transection resulted in lesions that were typical of OA in other species. Although lesions in both groups were generally uniform, those of the PMM model were more severe. Thus, both rat models provide a useful adjunct to study etiopathogenesis and therapeutic efficacy of drugs for treatment of OA.

References

1. **Altman, R. D., and D. D. Dean.** 1990. Osteoarthritis research: animal models. Semin. Arthritis Rheum. **19**(Suppl.1)**:**21-25.
2. **Oegema, T. R., Jr., and D. Visco.** 1999. Animal models of osteoarthritis, p. 349-367. *In* Y. H. An, R. J. Friedman, (ed.), Animal models in orthopaedic research. CRC Press, New York.
3. **Pritzker, K. P. H.** 1994. Animal models for osteoarthritis: processes, problems and prospects. Ann. Rheum. Dis. **53:**406-420.
4. **Troyer. H.** 1982. Experimental models of osteoarthritis: a review. Semin. Arthritis Rheum. **11:**362-374.
5. **Williams, J. M., D. L. Felten, R. G. Petersen, and B. L. O'Connor.** 1982. Effects of surgically induced instability on rat knee articular cartilage. J. Anat. **134:**103-109.
6. **Evans, E. B., G. W. N. Eggers, J. K. Butler, and J. Blumel.** 1960. Experimental immobilization and remobilization of rat knee joints. J. Bone Joint Surg. **42A:**737-758.
7. **Smale, G., A. Bendele, and W. E. Horton, Jr.** 1995. Comparison of age-associated degeneration of articular cartilage in wistar and fischer 344 rats. Lab. Anim. Sci. **45:**191-194.

8. **Sokoloff, L., and G. E. Jay, Jr.** 1956. Natural history of degenerative joint disease in small laboratory animals: 4. degenerative joint disease in the laboratory rat. A.M.A. Arch. Pathol. **62:**140-142.
9. **Moskowitz, R. W., W. Davis, J. Sammarco, M. Martens, J. Baker, M. Mayor, A. H. Burstein, and V. H. Frankel.**1973. Experimentally induced degenerative joint lesions following partial meniscectomy in the rabbit. Arthritis Rheum. 16:397-405.
10. **Pond, M. J., and G. Nuki.** 1973. Experimentally-induced osteoarthritis in the dog. Ann. Rheum. Dis. **32:**387-388.
11. **Gilbertson, E. M. M.** 1975. Development of periarticular osteophytes in experimentally induced osteoarthritis in the dog. A study using microradiographic, microangiographic, and fluorescent bone-labeling techniques. Ann. Rheum. Dis. **34:**12-25.
12. **Brandt, K. D., E. M. Braunstein, D. M. Visco, and B. L. O'Connor.** 1991. Anterior (cranial) cruciate ligament transection in the dog: a bona fide model of osteoarthritis, not merely of cartilage injury and repair. J. Rheumatol. **18:**436-46.
13. **Moskowitz, R. W.** 1984. Experimental models of osteoarthritis, p.109-128. *In* R. W. Moskowitz, D. S. Howell, V. M. Goldberg, H. J. Mankin (ed.), Osteoarthritis: diagnosis and management. W.B. Saunders Co., Philadelphia.
14. **Vidinov, N., V. Vasilev, F. Keller, W. Wolff, and G. Leutert**. 1990. Changes in the distribution of proteinpolysaccharide complexes within the articular cartilage in the experimental osteoarthrosis. Z. Mikrosk-Anat. Forsch. **104:**141-146.
15. **Hunziker, E. B.** 1992. Articular cartilage structure in humans and experimental animals, p.183-199. *In* K. E. Keuttner, R. Schleyerbach, J. G. Peyron, and V. C. Hascall (ed.), Articular cartilage and osteoarthritis. Raven Press, New York.
16. **Stockwell, R. A.** 1971. The interrelationship of cell density and cartilage thickness in mammalian articular cartilage. J. Anat. **109:** 411-421.
17. **Kiss. I., and I. Földes.** 1983. Effects of experimental patellar luxation on the knee joints in the rat. Acta. Morph. Hung. **31:**371-385.
18. **Gyarmati, J., I. Földes, M. Kern, and I. Kiss.** 1987. Morphological studies on the articular cartilage of old rats. Acta. Morph. Hung. **35:**111-124.
19. **Van Sickle, D. C., and S. A. Kincaid.** 1978. Comparative arthrology, p.1-47. *In* L. Sokoloff, (ed.), The joint and synovial fluid. Academic Press, New York.
20. **Thaxter, H. T., R. A. Mann, and C. E. Anderson.**1965. Degeneration of immobilized knee joints in rats: histological and autoradiographic study. J. Bone Joint Surg. **47A:**567-585.
21. **Aydelotte, B. M., B. L. Schumacher, and K. E. Kuettner.** 1992. Heterogeneity of articular cartilage, p.237-249. *In* K. E. Keuttner, R. Schleyerbach, J. G. Peyron, and V. C. Hascall (ed.), Articular cartilage and osteoarthritis. Raven Press, New York.
22. **Pedersen, H. E.** 1949. The ossicles of the semilunar cartilages of rodents. Anat. Rec. **105:**1-9.
23. **McDevitt, C. A., and R. R. Miller.** 1989. Biochemistry, cell biology, and immunology of osteoarthritis. Curr. Opin. Rheum. **1:**303-314.
24. **Dijkgraaf, L. C., L. G. M. De Bont, G. Boering, and R. S. B. Liem.** 1995. The structure, biochemistry, and metabolism of osteoarthritic cartilage: a review of the literature. J. Oral Maxillofac. Surg. **53:**1182-1192.
25. **Brandt, K. D.** 1993. Compensation and decompensation of articular cartilage in osteoarthritis. Agents Actions **40:**232-234.
26. **Oni, O. O. and I. Boyd.** 1998. The origin(s) of the periarticular osteophytes of osteoarthritic knee joints. Afr. J. Med. Med. Sciences **27:**23-25.
27. **Okazaki, K., S. Jingushi, T. Ikenoue, K. Urabe, H. Sakai, A. Ohtsuru, K. Akino, S. Yamashita, S. Nomura, and Y. Iwamoto.** 1999. Expression of insulin-like growth factor I messenger ribonucleic acid in developing osteophytes in murine experimental osteoarthritis in rats inoculated with growth hormone-secreting tumor. Endocrinology **140:**4821-4830.
28. **Horn, C. A., J. D. Bardley, K. D. Brandt, D. L. Kreipke, D. S. Slowman, and L. A. Kalasinski.** 1992. Impairment of osteophyte formation in hyperglycemic patients with type II diabetes mellitus and knee osteoarthritis. Arthritis Rheum. **35:**336-342.
29. **Kaiki, G., H. Tsuji, T. Yonezawa, H. Sekido, T. Takano, S. Yamashita, N. Hirano, and A. Sano.** 1990. Osteoarthrosis induced by intra-articular hydrogen peroxide injection and running load. J. Orthop. Res. **8:**731-740.
30. **Myers, S. L., K. D. Brandt, and O. Eilam.** 1995. Even low-grade synovitis significantly accelerates the clearance of protein from the canine knee. Implication for measurement of synovial fluid "markers" of osteoarthritis. Arthritis Rheum. **38:**1085-1091.
31. **Rumph, P. F., S. A. Kincaid, D. K. Baird, J. R. Kammermann, D. M. Visco, L. F. Goetze.** 1993. Vertical ground reaction force distribution during experimentally induced acute synovitis in dogs. Am. J. Vet. Res. **54:**365-369.
32. **Havelka, S., V. Horn, D. Spohrova, and P. Valouch.** 1984. The calcified-noncalcified cartilage interface: the tidemark. Acta. Biologica. Hung. **35:**271-279.
33. **Ostergaard, K., J. Petersen, C. B. Andersen, K. Bendtzen, D. M. Salter.** 1997. Histologic/histochemical grading system for osteoarthritic articular cartilage: reproducibility and validity. Arthritis Rheum. **40:**1766-1771.
34. **Van der Sluijs, J. A., R. G. T. Geesink, A. J. Van der Linden, S. K. Bulstra, R. Kuyer, and J. Drukker.** 1992. The reliability of the Mankin score for osteoarthritis. J. Orthop. Res. **10:**58-61.
35. **Campbell, C. J.** 1969. The healing of cartilage defects. Clin. Orthop. Rel. Res. **64:**45-63.
36. **Radin, E. L., and D. B. Burr**.1984. Hypothesis: joints can heal. Semin. Arthritis Rheum. **13:**293-302.
37. **Hunziker, E. B., and L. C. Rosenberg.** 1996. Repair of partial-thickness defects in articular cartilage: cell recruitment from the synovial membrane. J. Bone Joint Surg. **78-A:**721-733.
38. **Shapiro, F., S. Koide, and M. J. Glimcher**. 1993. Cell origin and differentiation in the repair of full-thickness defects of articular cartilage. J. Bone Joint Surg. **75-A:**532-553.